ANALYTICAL SCIENCES AUGUST 2010, VOL. 26

Chemical Effects of $CeL_{\gamma 4}$ Emission Spectra for Ce Compounds

Hisashi HAYASHI,*† Yuki TAKEHARA,* Naomi KAWAMURA, and Masaichiro MIZUMAKI****

**Department of Chemical and Biological Sciences, Faculty of Science, Japan Women's University, 2-8-1 Mejirodai, Bunkyo, Tokyo 112–8681, Japan*
***SPring-8, JASRI, 1-1-1 Kouto, Sayo-cho, Sayo, Hyogo 679–5198, Japan*

High-resolution $CeL_{\gamma 4}$ emission spectra of CeF_3, Ce_2S_3, CeF_4, and CeO_2 have been measured using a multicrystal, multidetector spectrometer. The spectra exhibited substantial differences depending on the chemical environment of the Ce ions. By comparing the observed CeO_2 spectrum with the band calculations, we determined that the observed chemical effects of the main emission line were primarily attributable to the transitions of the Ce5p band; the high-energy tail at around 6.539 keV was assigned to the ligand p→Ce2s cross transition. Further, a key difference between $CeL_{\gamma 4}$ and $EuL_{\gamma 4}$ is discussed with reference to CeL_1- and EuL_1-X-ray absorption fine-structures (XAFS). Possible applications of $CeL_{\gamma 4}$ emissions to material characterization are also suggested.

(Received April 10, 2010; Accepted June 24, 2010; Published August 10, 2010)

Introduction

Lanthanide compounds often exhibit remarkable optical, electrical, and magnetic properties. Mixed valencies and changes in the valence band structure play crucial roles in determining these properties. The valence states of lanthanide compounds strongly depend on their chemical environment. Therefore, information about the local electronic structures around the ions of interest is important in the various applications of lanthanide materials.

To analyze the electronic states of lanthanide samples, many spectroscopic techniques have been widely used, *e.g.*, optical absorption, electron spin resonance, Mössbauer spectroscopy, photoemission spectroscopy, and X-ray absorption fine-structure (XAFS) spectroscopy. Each of these techniques affords certain advantages and disadvantages. For example, valence band photoemission presents the most direct means of investigating the relevant electron configuration; however, it is non-element selective and is surface-sensitive, and it requires high-vacuum conditions. Thus, the development of new experimental probes as well as a combined use of the existing methods is important in the analytical studies of lanthanide materials.

Variations in the fine features of X-ray emission spectra in accordance with chemical combinations or chemical effects have been widely applied as nondestructive bulk probes for investigating low-Z materials ($Z < 30$).[1,2] Chemical effects provide unique information, complementary to that given by XAFS spectroscopy, about the local electronic and geometric structures of the elements of interest. To the best of our knowledge, the application of chemical effects to lanthanide compounds, despite their advantages, was not reported until 2009.[3,4] This is because the chemical effects in these compounds, particularly those caused by inner shell→core emissions, are minor. In contrast, the intensities of outer shell→core emissions, which are intrinsically low, exhibit relatively major chemical effects. The problem of low-intensity emissions is being overcome through current developments in multicrystal spectrometers[5–8] that are used with synchrotron X-ray sources.

In very recent studies,[3,4] we detected a large chemical shift (~5 eV) in the $EuL_{\gamma 4}$ (Eu5p→Eu2s) emission line. The $L_{\gamma 4}$ emission line (as well as other similar weak lines of lanthanides) has not been focused upon in modern X-ray studies. In this paper, we describe the chemical effects of $CeL_{\gamma 4}$ (Ce5p→Ce2s) emission and discuss its applicability to the characterization of Ce materials. This study will be the first step toward the extensive use of $L_{\gamma 4}$ emissions as a practical probe for an analysis of the chemical states of lanthanides.

Experimental

Chemicals

We obtained CeF_3, CeO_2, EuF_3, $EuCl_3$, and Eu_2O_3 from Wako Pure Chemical Industries Ltd.; Ce_2S_3 and CeF_4 from Alfa Aesar; and EuS from Kojundo Chemical Laboratory Co., Ltd. These commercially available chemicals with 3-N purity were compressed into pellets and used in our experiments without further purification.

Apparatus and measurements

$CeL_{\gamma 4}$ measurements were performed using a multicrystal, multidetector spectrometer.[5,6] This spectrometer, a schematic of which is shown in Fig. 1, was originally constructed in order to measure resonant inelastic X-ray scattering,[5] and it has only very recently been employed for $EuL_{\gamma 4}$ detection.[3] Basically, it consists of seven pairs of spherically bent crystals (bending radius: 820 mm) and a detector. All the crystals are placed such that their scattering angles are 135°. Emission spectra are measured by rotating the crystals and linearly moving the detectors simultaneously. Signals from each detector are fed

† To whom correspondence should be addressed.
E-mail: hayashih@fc.jwu.ac.jp

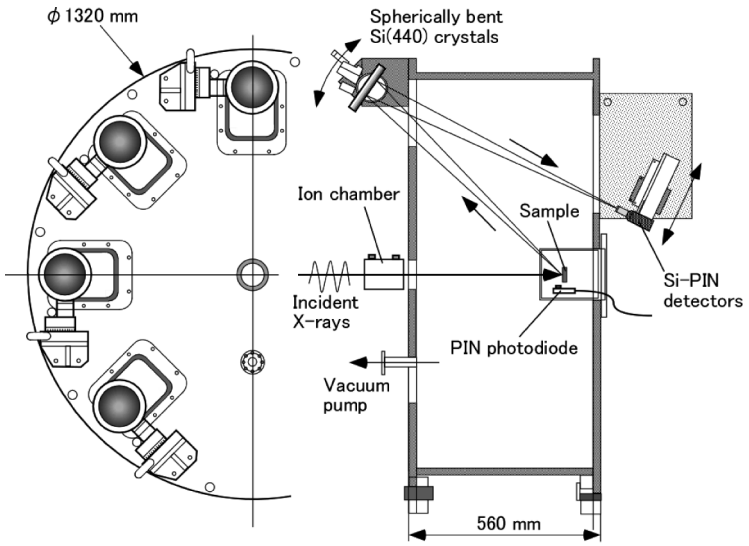

Fig. 1 Schematic layout of multicrystal, multidetector spectrometer.

into separate photon-counting electronics. Scintillation counters, which had been used as detectors in previous measurements,[3-6] were replaced by Si-PIN detectors (Amptek, XR-100T) in order to reduce the background caused by parasitic scatterings.

A sample is mounted in the multicrystal, multidetector spectrometer such that its surface faces the incoming beam. This ensures that both the horizontal and the vertical movements of the sample along its flat surface do not change the position of the source with respect to the spectrometer. Thus, the emitted X-ray energy is not sensitive to the position of the sample, and radiation damages can be minimized by selecting different positions of the sample without calibrating the energy frequently.

In the present experiments, we employed five spherically bent Si(440) crystals (diameter: 75 mm) as the analyzer crystals of the spectrometer. These crystals, obtained from Saint-Gobain, were prepared by gluing flat, polished 0.3 mm-thick wafers onto spherical glass holders. In order to achieve high energy resolution, we operated the analyzer crystals close to backscattering geometry, and we covered the Bragg angles ranging from 72° to 82°; these correspond to an energy range of 6.52 – 6.79 keV. In this alignment, a solid angle of approximately 0.033 sr was subtended.

The $CeL_{\gamma 4}$ data were collected using the hard X-ray undulator beamline BL39XU at SPring-8, Hyogo, Japan. This beamline consists of a dispersive diamond (111) double crystal monochromator and a rhodium-coated cylindrically bent mirror to focus the beam horizontally. The photon flux at the sample position was estimated to be approximately 1×10^{13} photons/s, and it was monitored using an ion chamber placed in front of the spectrometer. The spot size on the sample was 0.3 mm (height) × 0.1 mm (width). The spectrometer was mounted on a computer-controlled *X*-*Z* stage in alignment with the beam. The beam path has 50 μm-thick Kapton windows, and it was evacuated using a scroll pump to avoid the absorption and scattering of the photons by air.

Under the above-mentioned conditions, the overall energy resolution (energy resolution of monochromator + analyzers) as estimated from the FWHM of the elastic line was 0.6 eV at 6.528 keV. The $CeL_{\gamma 4}$ emission spectra were measured from 6.517 to 6.5444 keV at intervals of 0.2 eV. To the best of our knowledge, this is the first high-resolution measurement of $CeL_{\gamma 4}$ emission spectra.

L_1-XAFS spectra of the Ce and Eu samples were obtained by monitoring the intensities of the total fluorescent X-rays near the sample by using a PIN photodiode during the scanning of the excitation energy. All the measurements were performed at room temperature.

Theoretical Calculations

The $CeL_{\gamma 4}$ emission profile of CeO_2 was obtained from full-potential augmented-plane-wave (APW) band structure calculations under the generalized gradient approximation using the WIEN2k code.[9,10] In these calculations, CeO_2 was considered to have a CaF_2 arrangement (cell edge: 5.411 Å). Here, a $2 \times 2 \times 2$ supercell was constructed, and one Ce2s electron was removed to produce core hole effects. The total number of k points in the entire Brillouin zone was 1000. After the convergence of the self-consistency cycle in the calculation, valence p→Ce2s emission was calculated using the XSPEC software in the WIEN2k package. Here, the spectrum of dipole-allowed transitions was calculated by generating matrix elements, which were multiplied by a radial transition probability and the partial densities of states of CeO_2. The calculated emission lines were broadened using Lorentz functions whose FWHMs were 5.7 eV; this value corresponded to both experimental and core level broadenings.

Results and Discussion

Figure 2 shows $CeL_{\gamma 4}$ spectra of CeF_3, Ce_2S_3, CeF_4, and CeO_2. All spectra were measured at an excitation energy of 6.630 keV. The spectra differ substantially depending on the chemical environment of the Ce ions. Such results are common for low-*Z* materials (especially for $Z < 18$),[1,2] but not necessarily for lanthanide compounds.[11] The chemical effects studied here indicate that, with the help of systematically accumulating spectral data of reference compounds, highly resolved $CeL_{\gamma 4}$ emission can be used to identify the valence states and local geometry (such as the species of ligands along with their interatomic distances, bond angles, and number of ligands) of Ce.

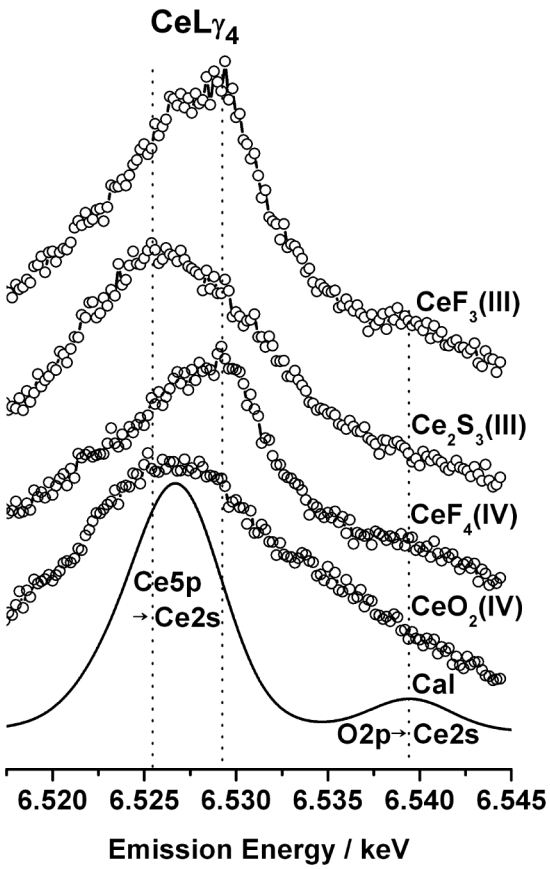

Fig. 2 $CeL_{\gamma4}$ spectra of CeF_3, Ce_2S_3, CeF_4, and CeO_2. Calculated $CeL_{\gamma4}$ spectrum of CeO_2 ("Cal") is also shown. Dotted lines help correlation.

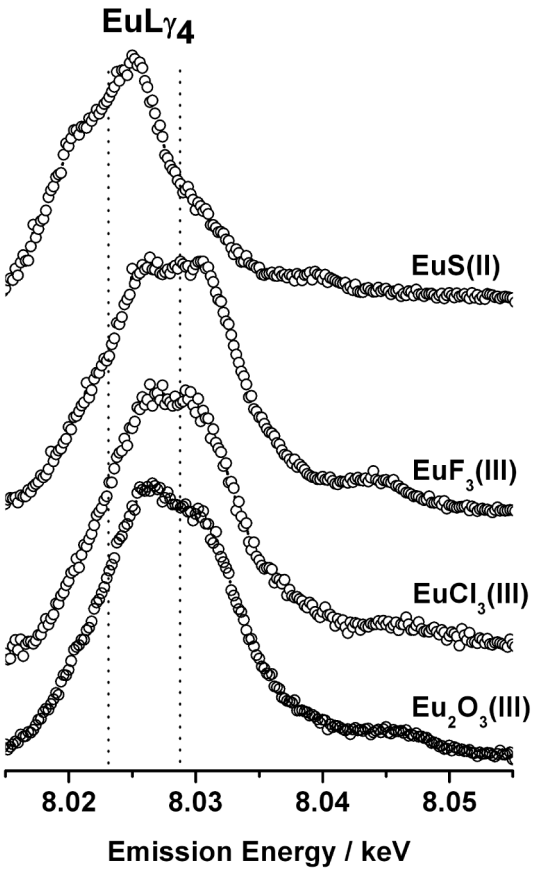

Fig. 3 $EuL_{\gamma4}$ spectra of EuS, EuF_3, $EuCl_3$, and Eu_2O_3 (Ref. 3). Dotted lines help correlation.

Figure 2 also shows valence p→Ce2s emission spectra of CeO_2 calculated using the APW band calculation performed by the WIEN2k code. This calculation takes into account the band effects of Ce5p in the initial ($Ce2s^{-1}$) state, but it does not take into account the final ($Ce5p^{-1}$) state multiplets. Therefore, it is expected that the calculated profile will not be identical to the experimental CeO_2 spectrum. However, the WIEN2k calculation provides the following significant insights into the fundamental properties of the observed emissions. First, the calculated profile reproduces the overall shape of the experimental spectra. This fairly good agreement between the two profiles suggests that the $CeL_{\gamma4}$ profile is governed by the property of the p-type valence band, making it possible to assign the main peak fundamentally to Ce5p→Ce2s, as expected. Such strong influence of the valence band is not very common in the L_γ emissions of lanthanides. For example, Ohno and LaVilla reported the breakdown of the one-electron band picture in the $L_{\gamma2,3}$ (4p→2s) spectra of Sm_2O_3 and Nd_2O_3 to generate a very broad low-energy structure having a width of ~60 eV.[12] Such a structure was not observed in our study. The broadening of the $L_{\gamma2,3}$ lines was interpreted in terms of the strong configuration interaction (CI) between the 4p single hole state and 4d double hole states.[12] For Ce, 5p electrons belong to the outer shells and contribute to the valence band; the resultant minor CI effects caused by the inner shell electrons can make the valence band nature dominant in $CeL_{\gamma4}$, as shown in Fig. 2. Second, the high-energy tail at around 6.539 keV is basically attributable to the cross transitions from the valence O2p orbital to the Ce2s hole. Because the atomic binding energies of F2p (9 eV), S3p (8 eV), and O2p (7 eV) are similar, the hump observed at around 6.539 keV for other Ce samples can also be assigned to such cross transitions to the first approximation. As shown in Fig. 2, the experimental $CeL_{\gamma4}$ linewidth of CeO_2 is significantly broader than that of other compounds. Because of strong Ce4f-O2p hybridization, the mixed valence of CeO_2[13] may be responsible for the line broadening. Further detailed calculations are required to interpret the CeO_2 profile more quantitatively.

For comparison with the $CeL_{\gamma4}$ results, $EuL_{\gamma4}$ spectra[3] of EuS, EuF_3, $EuCl_3$, and Eu_2O_3 are shown in Fig. 3. They are the only available reference data to chemical effects of $L_{\gamma4}$ emission at present, and also interesting subjects of the comparison since Eu has half-filled 4f shell to show mixed valence. As reported previously,[3] the spectra of Eu compounds having the same oxidation number (Eu(III)) do not differ significantly, and the EuS profile exhibits a considerably large chemical shift of approximately 5 eV (estimated as the difference between the centers of the Eu(II) and Eu(III) bands). These Eu results are different from those for Ce. For example, in case of $CeL_{\gamma4}$, the peak positions of CeF_3 and Ce_2S_3 are evidently different, although their formal Ce oxidation numbers are the same. On the other hand, the peak positions of CeF_3 and CeF_4 are almost the same, although their oxidation numbers are different. These observations indicate that $CeL_{\gamma4}$ is influenced more strongly by the local geometry than by the oxidation number. Therefore, $CeL_{\gamma4}$ is less sensitive to the oxidation number than $EuL_{\gamma4}$.

Figures 4 and 5 show L_1-XAFS spectra of the Ce and Eu samples, respectively. Among the Eu compounds, the L_1-edge energies exhibit considerable differences for the Eu(II) and

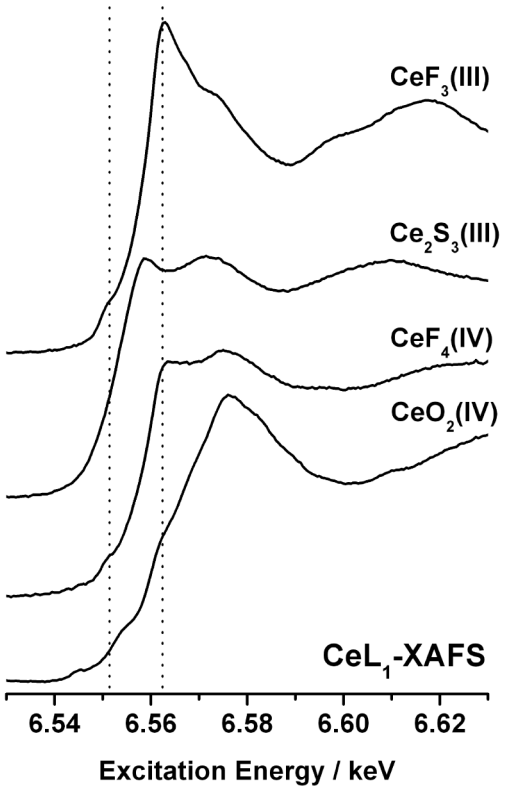

Fig. 4 CeL_1-XAFS spectra of CeF_3, Ce_2S_3, CeF_4, and CeO_2. Dotted lines help correlation.

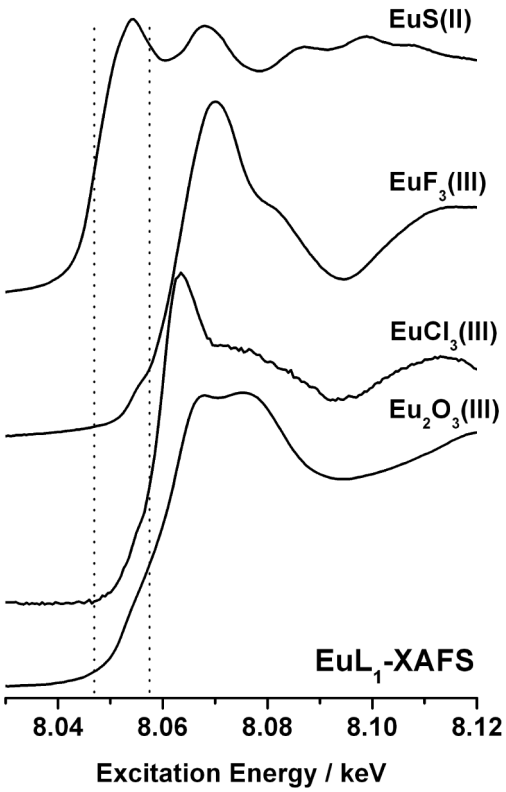

Fig. 5 EuL_1-XAFS spectra of EuS, EuF_3, $EuCl_3$, and Eu_2O_3. Dotted lines help correlation.

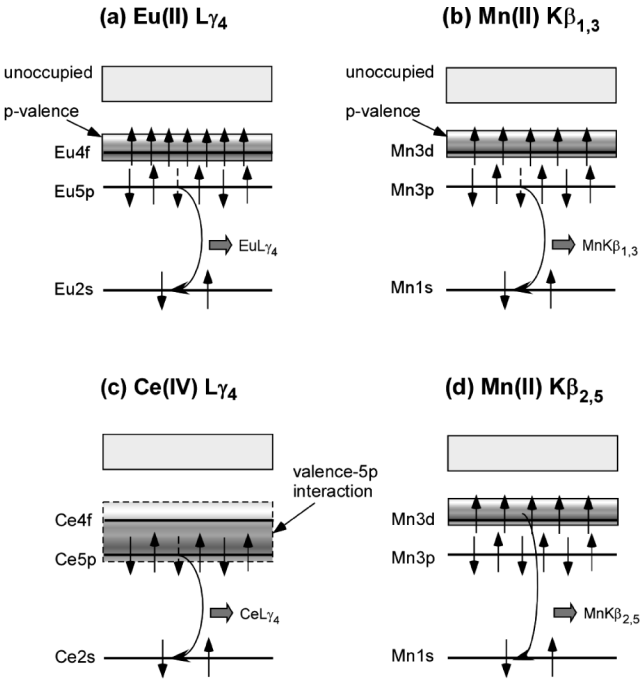

Fig. 6 Schematic representation of emissions for (a) Eu(II)$L_{\gamma 4}$, (b) Mn(II)$K_{\beta 1,3}$, (c) Ce(IV)$L_{\gamma 4}$, and (d) Mn(II)$K_{\beta 2,5}$.

the Eu(III) compounds (approximately 10 eV); however, such noticeable differences are not observed among the Eu(III) compounds (a few electron volts). On the other hand, the valence dependence of the L_1-edge energies among the Ce compounds is not straightforward. For the same formal oxidation number, the L_1-edge energy differs considerably depending on the ligands, *e.g.*, the edge energy of CeF_3 is higher than that of Ce_2S_3 by approximately 6 eV. These results of the L_1-edge energies are consistent with those of the $L_{\gamma 4}$ spectra of Ce and Eu, suggesting that the valence dependence of the $L_{\gamma 4}$ emissions is dominated by that of the L_1-edge energies.

In a previous study,[3] we pointed out the similarity between the mechanisms for the $L_{\gamma 4}$ emission of Eu and the $K_{\beta 1,3}$ emission of Mn or Fe. As shown in Figs. 6a and 6b, both of these emissions are accompanied by transitions from an "inner" p shell (approximately a few dozen of electron volts below the Fermi level) to an "inner" s core, and in both emissions, highly localized orbitals (4f or 3d) are present immediately above the resultant p holes (5p or 3p). Transitions between core levels can be effectively used to separate structural changes from the charge density ones, because the transitions are expected to be largely independent of the electronic structure in the valence band. The chemical sensitivity of the core level transitions generally arises from either screening effects or electron-electron interaction. The $K_{\beta 1,3}$ lines in 3d transition metal ions[13–16] and the $EuL_{\gamma 4}$ lines[3] are dominated by 3p–3d and 5p–4f exchange interactions, respectively. Consequently, both these lines are sensitive also to the local spin states.

On the other hand, a small number of 4f electrons (0 or 1) in Ce compounds weaken the intra-atomic 5p–4f interaction and can promote interactions between 5p and the valence band. Thus, the $L_{\gamma 4}$ emission (5p→2s) can reflect the nature of the p-type valence band more sensitively. The resultant situation is similar to the situation of the $K_{\beta 2,5}$ satellites (valence p→1s) of 3d transition metals[13,17] (Figs. 6c and 6d). It is generally accepted that the shape of valence p→1s emissions during a

change in the oxidation state is influenced by (i) changes in local structure, which lead to the formation of new molecular orbitals, and (ii) changes in the metal-ion charge.[18] Therefore, the $K_{\beta 2,5}$ spectra of 3d elements are often only indirectly sensitive to the formal valence of the elements, and orbital hybridizations may lead to only small spectral differences in the case of changes in the formal oxidation number.[18] The present $CeL_{\gamma 4}$ results (Fig. 2) are in good agreement with the nature of $K_{\beta 2,5}$, as described above. Such $CeL_{\gamma 4}$ may not help in determining the formal oxidation numbers, but it can be used in examining the interplay between structural and electronic changes.

The high-energy tail region at around 6.539 keV is particularly interesting with regard to the characterization of Ce materials using $CeL_{\gamma 4}$ emission. This region is considered to be sensitive to the "hybridization" between Ce5p and ligand p (Fig. 2), which, in turn, depends on the extent of the charge transfer (CT) from the ligand to the Ce ions. For systems in which the CT effects are of prime importance, such as CeB_6,[19,20] a detailed analysis of this tail region can provide clues to the problem.

In addition, cases in which only selective energies are available for excitation have an advantage in that $CeL_{\gamma 4}$ measurements (as well as other X-ray emission measurements) do not require an incident energy scan. This advantage may become important when X-ray laser sources enter the phase of practical application.

Acknowledgements

We thank Ms. M. Katagiri (Japan Women's Univ.) for her assistance in the $CeL_{\gamma 4}$ measurements. The experiments discussed in this paper were carried out at SPring-8, Hyogo, Japan under proposals 2008A1336, 2009A1186, and 2009A1187. This study was supported by a Grant-in-Aid for Scientific Research (B) (No. 20350039) from the Ministry of Education, Culture, Sports, Science and Technology (MEXT), Japan.

References

1. B. K. Agarwal, "*X-Ray Spectroscopy*," **1989**, Springer-Verlag, New York.
2. A. A. Markowicz, "*Handbook of X-Ray Spectrometry*," ed. R. E. Van Grieken and A. A. Markowicz, **2002**, Marcel Dekker, New York.
3. H. Hayashi, N. Kawamura, M. Mizumaki, and T. Takabatake, *Anal. Chem*., **2009**, *81*, 1522.
4. H. Hayashi, N. Kawamura, M. Mizumaki, T. Takabatake, H. Imura, K. Okamoto, and T. Akai, *J. Phys. Conference Series*, **2009**, *190*, 012050.
5. H. Hayashi, *Anal. Sci*., **2008**, *24*, 15.
6. H. Hayashi, T. Azumi, A. Sato, and Y. Udagawa, *J. Electron Spectrosc. Relat. Phenom*., **2008**, *168*, 34.
7. U. Bergmann and S. P. Cramer, *SPIE Proc*., **1998**, *3448*, 198.
8. H. Hayashi, M. Kawata, R. Takeda, Y. Udagawa, Y. Watanabe, T. Takano, S. Nanao, and N. Kawamura, *J. Electron Spectrosc. Relat. Phenom*., **2004**, *136*, 191.
9. P. Blaha, K. Schartz, P. Sorantin, and S. B. Trickey, *Comput. Phys. Commun*., **1990**, *59*, 399.
10. P. Blaha, K. Schwarz, G. Madsen, D. Kvasnicka, and J. Luitz, http://www.wien2k.at/.
11. G.-Z. Shi, K. Fujisawa, T. Konishi, S. Fukushima, A. Iida, and Y. Gohshi, *Adv. X-ray Chem. Anal. Jpn*. (in Japanese), **1986**, *18*, 181.
12. M. Ohno and R. E. LaVilla, *Phys. Rev. B*, **1989**, *39*, 8852.
13. F. M. F. de Groot and A. Kotani, "*Core Level Spectroscopy of Solids*," **2008**, Taylor and Francis, New York.
14. X. Wang, F. M. F. de Groot, and S. P. Cramer, *Phys. Rev. B*, **1997**, *56*, 4553.
15. P. Glatzel, U. Bergmann, J. Yano, H. Visser, J. H. Robblee, W. W. Gu, F. M. F. de Groot, G. Christou, V. L. Pecoraro, S. P. Cramer, and V. K. Yachandra, *J. Am. Chem. Soc*., **2005**, *126*, 9946.
16. G. Vanko, T. Neisius, G. Molnar, F. Renz, S. Karpati, A. Shukla, and F. M. F. de Groot, *J. Phys. Chem*., **2006**, *110*, 11647.
17. U. Bergmann, C. R. Horne, T. J. Collins, J. M. Workman, and S. P. Cramer, *Chem. Phys. Lett*., **1999**, *302*, 119.
18. P. Glatzel, G. Smolentsev, and G. Bunker, *J. Phys. Conference Series*, **2009**, *190*, 012046.
19. M. Magnuson, S. M. Butorin, J.-H. Guo, A. Agui, J. Nordgren, H. Ogasawara, A. Kotani, T. Takahashi, and S. Kunii, *Phys. Rev. B*, **2001**, *63*, 075101.
20. K. Tanaka, Y. Kato, and Y. Onuki, *Acta Crystallogr*., **1997**, *B53*, 143.